On the Dimensionality of the Reaction Coordinate of Intramolecular Charge-Transfer Reactions in Protic Solvents†

John D. Simon* and Robert Doolen

Contribution from the Department of Chemistry, University of California at San Diego, La Jolla, California 92093-0341. *Received August 19, 1991. Revised Manuscript Received February 27, 1992*

Abstract: Steady-state and time-resolved emission spectroscopies are used to examine the kinetics of intramolecular charge transfer in a series of bis[(*N*,*N*-dialkylamino)phenyl]sulfones in polar solvents. The experimental data are compared to theoretical models to determine the nature of the reaction coordinate. The steady-state emission spectra are compared to calculated spectra by using the solvent coordinate model developed by Barbara and co-workers (*Chem. Phys.* **1990**, *149*, 81). This model is unable to quantitatively describe the steady-state spectra, indicating that a reaction coordinate that depends on solvation alone does not account for the reaction process in this set of molecules. Comparison of the experimental data to the kinetic model of Sumi, Nadler, and Marcus (*J. Chem. Phys.* **1986**, *84*, 4804; **1987**, *86*, 3906) suggests that the reaction process is controlled by fluctuations in the intramolecular modes, followed by relaxation in the surrounding solvent. Within this theoretical model, the nonexponentiality of the decays of the reactant population and the various moments of these decays can be quantitatively accounted for. Although the molecular nature of the vibrational modes that are coupled to the reaction process remain elusive, these results indicate the importance of considering a multidimensional model in describing activated electron transfer reactions in polar solvents.

Introduction

Electron-transfer reactions play an important role in many chemical and biological processes. It is now well established that the solvent plays an important role in determining the activation parameters and free energies of the reactants and products through static interactions. In particular, the role of the solvent in determining energetic factors of the reaction forms the basis of Marcus theory[1] and several other related kinetic models for charge-transfer reactions.[2] These theoretical models have been very successful in describing many experimental systems, indicating that, in many cases, the role of the solvent on the reaction rate can be understood in terms of changes in the potential energy surface induced by the static dielectric interactioins of the reacting molecule(s) with the solvent. In the past decade, it has been realized that the solvent can also play a dynamic role in charge-transfer processes.[3-11] This solvent friction has received extensive theoretical attention,[12] but only in the last 5 years have detailed experiments been reported that address the importance of solvation dynamics in charge-transfer reactions.[13] Unlike static dielectric effects, the dependence of the rate of change transfer on solvent dynamics is generally manifested by a dependence of the prefactor of the kinetic expression on time scales associated with the motion of the solvent. Unfortunately, at present, the exact relationship between the prefactor and solvent relaxation times is model dependent.

In order to understand the role of solvent dynamics in charge-transfer reactions, the time scales for solvent relaxation need to be determined. Data from dielectric loss spectroscopy, combined with continuum dielectric models of the solvent, have been extensively used to determine solvent relaxation times.[14] In particular, the longitudinal relaxation time,[15] τ_L, has been used to gauge solvent dynamics pertinent to electron-transfer reactions. Although some electron-transfer reactions exhibit rate constants that correlate with (or are equal to) τ_L,[16] a large number of reactions exhibit rate constants that are faster than τ_L^{-1}.[17] These latter cases have been treated in terms of contributions from vibrational effects, as the fastest solvent-controlled rate constant predicted by using a continuum description of the solvent is τ_L^{-1}. However, recent time-resolved studies of the dynamic Stokes shift of probe molecules in polar solvents reveal that solvation is generally characterized by a distribution of relaxation times.[18] These experimental studies focus on measuring the function $C(t)$,[8,19] given in eq 1. In this expression, $\nu(0)$, $\nu(t)$, and $\nu(\infty)$ are the maximum

$$C(t) = \frac{\nu(t) - \nu(\infty)}{\nu(0) - \nu(\infty)} \quad (1)$$

of the emission spectrum at time zero, time t, and full relaxation ($t \rightarrow \infty$). The evolution of $C(t)$ is related to solvent orientational

† This paper is dedicated to the memory of Teresa Fonseca.

(1) (a) Marcus, R. A. *J. Chem. Phys.* **1956**, *24*, 966. (b) Marcus, R. A. *Faraday Discuss. Chem. Soc.* **1960**, *29*, 21. (c) Marcus, R. A. *J. Chem. Phys.* **1963**, *38*, 1858. (d) Marcus, R. A. *Annu. Rev. Phys. Chem.* **1964**, *15*, 155.

(2) (a) Hush, N. S. *Trans. Faraday Soc.* **1961**, *57*, 557. (b) Hush, M. S. *J. Chem. Phys.* **1958**, *28*, 968. (c) Sutin, N. *Acc. Chem. Res.* **1982**, *15*, 275. (d) Levich, V. G. *Adv. Electronchem. Electrochem. Eng.* **1966**, *4*, 249.

(3) (a) Newton, M. D.; Friedman, H. L. *J. Chem. Phys.* **1988**, *88*, 4460. (b) Newton, M. D.; Sutin, N. *Annu. Rev. Phys. Chem.* **1984**, *35*, 437.

(4) (a) Calef, D. F.; Wolynes, P. G. *J. Phys. Chem.* **1983**, *87*, 3381. (b) Calef, D. F.; Wolynes, P. G. *J. Chem. Phys.* **1983**, *78*, 470.

(5) (a) Warhsel, A. *J. Phys. Chem.* **1982**, *86*, 2218. (b) Warshel, A.; Russell, S. T.; Sussman, F. *Isr. J. Chem.* **1987**, *27*, 217. (c) Hwang, J.-K.; Warshel, A. *J. Am. Chem. Soc.* **1987**, *109*, 715. (d) Hwang, J.-K.; King, G.; Creighton, S.; Warshel, A. *J. Am. Chem. Soc.* **1988**, *101*, 5297.

(6) (a) Sumi, H.; Marcus, R. A. *J. Chem. Phys.* **1986**, *84*, 4894. (b) Nadler, W.; Marcus, R. A. *J. Chem. Phys.* **1987**, *86*, 3906.

(7) (a) Zusman, L. D. *Chem. Phys.* **1980**, *49*, 295. (b) Zusman, L. D. *Chem. Phys.* **1983**, *80*, 29. (a) Zusman, L. D. *Chem. Phys.* **1988**, *119*, 51.

(8) van der Zwan, G.; Hynes, J. T. *J. Phys. Chem.* **1985**, *89*, 4181.

(9) (a) Rips, I.; Jortner, J. *J. Chem. Phys.* **1987**, *87*, 2090. (b) Rips, I.; Jortner, J. *J. Chem. Phys.* **1987**, *87*, 6513. (c) Rips, I.; Jortner, J. *J. Chem. Phys.* **1988**, *88*, 818.

(10) (a) Sparpaglione, M.; Mukamel, S. *J. Chem. Phys.* **1988**, *88*, 3266. (b) Sparpaglione, M.; Mukamel, S. *J. Chem. Phys.* **1988**, *88*, 4300. (c) Sparpaglione, M.; Mukamel, S. *J. Chem. Phys.* **1988**, *88*, 1465. (d) Sparpaglione, M.; Mukamel, S. *J. Phys. Chem.* **1987**, *91*, 3938.

(11) (a) Fonseca, T. *J. Chem. Phys.* **1989**, *91*, 2869. (b) Fonseca, T. *Chem. Phys. Lett.* **1989**, *162*, 491.

(12) Hynes, J. T. *J. Phys. Chem.* **1986**, *90*, 3701.

(13) (a) Barbara, P. F.; Jarzeba, W. *Adv. Photochem.* **1990**, *15*, 1. (b) Maroncelli, M.; McInnis, J.; Fleming, G. R. *Science* **1988**, *243*, 1674. (c) Simon, J. D. *Acc. Chem. Res.* **1988**, *21*, 128. (d) Maroncelli, M. *J. Mol. Liquids*, in press.

(14) Garg, S. K.; Smyth, C. P. *J. Phys. Chem.* **1965**, *69*, 1294 and references therein.

(15) (a) Frohlich, H. Theory of Dielectrics. Oxford Univ., Oxford, 1949. (b) Friedman, H. *Trans. Faraday Soc.* **1983**, *79*, 1465 C9. Davies, M. In *Dielectric Properties and Molecular Behavior*; Hill, N., Vaughan, W. E., Price, A. H., Davies, M., Eds.; Van Nostrand: London, 1969.

(16) (a) Huppert, D.; Kosower, E. M. *Annu. Rev. Phys. Chem.* **1986**, *37*, 127. (b) Huppert, D.; Kanety, H.; Kosower, E. M. *Faraday Discuss. Chem. Soc.* **1982**, *74*, 161. (c) Kosower, E. M.; Dodiak, K.; Tanizawa, K.; Ottolenghi, M.; Orbach, N. *J. Am. Chem. Soc.* **1975**, *97*, 2167. (d) Kosower, E. M. *J. Am. Chem. Soc.* **1985**, *107*, 1114.

0002-7863/92/1514-4861$03.00/0

relaxation and provides a direct measure of the time dependence of dielectric friction.[8,19] In general, workers have focused on reporting an average solvation time, τ_s, which is given by the time integral of $C(t)$. Continuum dielectric theory predicts that $C(t)$ should decay exponentially with a time constant of τ_L. For a large variety of solvents and probe molecules, one finds that $\tau_s \approx \tau_L$.[13] However, it is important to stress that $C(t)$ is generally a *nonexponential* function, revealing a distribution of relaxation times, with components that are significantly faster than τ_L.

The nonexponential behavior of $C(t)$ is important, as several recent theoretical works indicate that the time scale of solvent motion relevant to the reaction process is related to the curvature of the potential energy surface at the barrier. In particular, Hynes and co-workers have developed frequency-dependent friction models for describing the coupling of the solvent to the reaction dynamics.[12] Computer simulations[20-24] also suggest that the average solvation time measured by the time integral of $C(t)$ may not be the relevant time scale of solvent fluctuations in electron-transfer reactions. It is necessary to consider the role of these fast solvation times on electron-transfer reactions. Experimentally, this issue has recently been addressed by Barbara, Weaver, and co-workers in accounting for anomalously fast reaction rates for exchange kinetics in a series of cobaltocenium–cobaltocene molecules in various polar solvents that exhibit fast components in their experimental $C(t)$ functions.[25]

Studies of excited-state intramolecular charge-transfer reactions reported by Barbara and co-workers reveal that, in certain cases, the reaction dynamics can be completely determined by solvent motion.[26] This conclusion was originally based on the observation that the first moments of the decay of the LE state of bianthryl in a series of polar aprotic solvents were similar to the average solvation times determined from $C(t)$ measurements of Coumarin probe molecules. More recently, Barbara and co-workers have developed a semiempirical model that enables one to calculate electronic absorption and emission spectra assuming that the excited-state reaction coordinate is described by solvent dielectric relaxation.[26] They show that the function $C(t)$ can be used to represent motion along this reaction coordinate. In the case of bianthryl (BA) and 4-(9-anthryl)-*N*,*N*'-dimethylaniline (ADMA), this model can quantitatively reproduce the solvent dependence of the experimental spectra as well as the population decays of the electronically excited reactant state. The details of these calculation will be discussed later in connection to the molecules studied in this paper. Studies on intermolecular electron-exchange reactions reported by Weaver and co-workers also support the conclusion that solvent dynamics can control the reaction rate.[27] These workers point out that, in interpreting the dynamical data, corrections to the activation energies resulting from changes in the solvent need to be accounted for. In the case of intramolecular charge-transfer reactions, this latter issue was first addressed by Eisenthal and co-workers.[28]

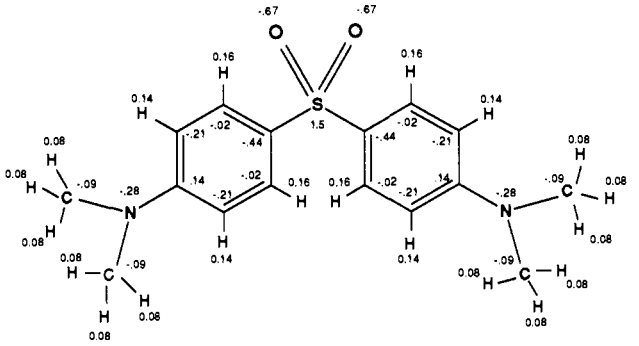

Figure 1. Charge distribution for the ground state of DMAPS calculated by using AM-1 are shown. The magnitude of the ground-state moment is 9.3 D.

Table I. Dipole Moments and Molecular Volumes of the Symmetric Sulfone Molecules Studied

molecule	μ_{gs},[a] D	volume,[b] Å^3	μ_{lici},[c] D
APS	9.3	128	16.0
DMAPS	9.5	170	17.0
DEAPS	8.8	225	18.1
DPAPS	8.8	266	19.7
DBAPS		397	

[a] Determined from MNDO calculations. [b] Determined from van der Waals radii given in ref 39. [c] Determined from combining the MNDO calculations with the Lippert–Mataga analysis of the steady-state emission and absorption spectra.

In addition to dynamic solvation effects, other factors can contribute to determine the reaction rate. In particular, Sumi, Nadler, and Marcus discussed the case where fluctuations in both the solvent and the intramolecular vibrational modes can lead to reaction.[6] Under certain conditions, vibrational fluctuations can dominate the total reorganization energy for electron-transfer reactions. In this limit, depending on the magnitude of the reaction free energy barrier, rate constants significantly faster than the inverse of the solvent relaxation times can be observed. In intermediate cases, where solvation and vibrational effects both contribute, the first moment of the reactant population decay, τ_a, may depend on τ_L in a power law form; $\tau_a \propto \tau_L^{\alpha}$ $(0 < \alpha \leq 1)$. Similar power-dependent relationships have also been suggested for strictly solvent-controlled reactions in non-Debye liquids.[29] In addition, quantum mechanical effects resulting from high-frequency vibrations of the donor and acceptor groups can determine the chemical reaction rate.[30] This later process, where the mathematical formulation is based on evaluation of Franck–

(17) (a) Su, S.-G.; Simon, J. D. *Chem. Phys. Lett.* **1989**, *158*, 423. (b) Kahlow, M. A.; Kang, T.-J.; Barbara, P. F. *J. Phys. Chem.* **1987**, *91*, 6452. (c) McManis, G. E.; Golovin, M. N.; Weaver, M. *J. Chem. Phys.* **1986**, *90*, 6563. (d) Akesson, E.; Walker, G. C.; Barbara, P. F. *J. Chem. Phys.*, submitted for publication. (e) Su, S.-G.; Simon, J. D. *J. Chem. Phys.* **1988**, *89*, 908. (f) Simon, J. D. *Pure Appl. Chem.* **1990**, *62*, 2243. (g) Simon, J. D.; Su, S.-G. *J. Phys. Chem.* **1990**, *94*, 3656.

(18) (a) Su, S.-G.; Simon, J. D. *J. Phys. Chem.* **1987**, *91*, 2693. (b) Kahlow, M. A.; Kang, T. J.; Barbara, P. F. *J. Chem. Phys.* **1988**, *88*, 2372. (c) Castner, E. W., Jr.; Maroncelli, M.; Fleming, G. R. *J. Chem. Phys.* **1987**, *86*, 1090. (d) Maroncelli, M.; Fleming, G. R. *J. Chem. Phys.* **1987**, *86*, 6221. (e) Chapman, C. F.; Fee, R. S.; Maroncelli, M. *J. Phys. Chem.* **1991**, *94*, 4929. (f) Rosenthal, S. J.; Xie, X.; Du, M.; Fleming, G. R. *J. Chem. Phys*, submitted for publication. (g) Simon, J. D.; Su, S.-G. *Chem. Phys.* **1991**, *152*, 143.

(19) Bagchi, B.; Oxtoby, D. W.; Fleming, G. R. *Chem. Phys.* **1985**, *86*, 257.

(20) (a) Gertner, B. J.; Whitnell, R. M.; Wilson, K. R.; Hynes, J. T. *J. Am. Chem. Soc.* **1991**, *113*, 74. (b) Gertner, B. J.; Wilson, K. R.; Hynes, J. T. *J. Chem. Phys.* **1989**, *90*, 3537.

(21) Borgis, D.; Hynes, J. T. *J. Chem. Phys.* **1991**, *94*, 3619.

(22) Warshel, A.; Hwang, J.-K. *J. Chem. Phys.* **1986**, *84*, 4938.

(23) Kuharski, R. A.; Bader, J. S.; Chandler, D.; Sprik, M.; Klein, M.; Impey, R. W. *J. Chem. Phys.* **1988**, *89*, 3248.

(24) Bader, J. S.; Chandler, D. *Chem. Phys. Lett.* **1989**, *157*, 501.

(25) Weaver, M. J.; McManis, G. E.; Jarzeba, W.; Barbara, P. F. *J. Phys. Chem.* **1990**, *94*, 1715.

(26) (a) Kang, T. J.; Kahlow, M. A.; Giser, D.; Swallen, S.; Nagarajan, V.; Jarzeba, W.; Barbara, P. F. *J. Phys. Chem.* **1988**, *92*, 6800. (b) Kang, T.-J.; Jarzeba, W.; Barbara, P. F.; Fonseca, T. *Chem. Phys.* **1990**, *149*, 81. (c) Tominaga, K.; Walker, G. C.; Jarzeba, W.; Barbara, P. F. *J. Phys. Chem.* **1991**, *95*, 10475. (d) Tominaga, K.; Walker, G. C.; Kang, T. J.; Barbara, P. F.; Fonseca, T. *J. Phys. Chem.* **1991**, *95*, 10485.

(27) (a) Weaver, M. J.; McManis III, G. E. *Acc. Chem. Res.* **1990**, *23*, 294. (b) McManis, G. E., III; Weaver, M. J. *J. Chem. Phys.* **1989**, *90*, 912. (c) McManis, G. E., III; Weaver, M. J. *J. Chem. Phys.* **1989**, *90*, 1720. (d) Gennett, T.; Milner, D. F.; Weaver, M. J. *J. Phys. Chem.* **1985**, *89*, 2787. (e) Nelson, R. M.; McManis, G. E., III; Weaver, M. J. *J. Phys. Chem.* **1988**, *93*, 4703. (f) Nelson, R. M.; McManis, G. E., III; Golovin, M. N.; Weaver, M. J. *J. Phys. Chem.* **1988**, *92*, 3441.

(28) (a) Wang, Y.; Eisenthal, K. B. *J. Chem. Phys.* **1982**, *77*, 6076. (b) Yang, Y. C.; McAuliffe, M. J.; Novak, F.; Eisenthal, K. B. *J. Phys. Chem.* **1981**, *85*, 3736. (c) Hicks, J. M.; Vandersall, M.; Barbarogic, Z.; Eisenthal, K. B. *Chem. Phys. Lett.* **1985**, *116*, 18. (d) Hicks, J. M.; Vandersall, M. T.; Sitzmann, E. V.; Eisenthal, K. B. *Chem. Phys. Lett.* **1987**, *135*, 413.

(29) Rips, I.; Jortner, J. *Chem. Phys. Lett.* **1987**, *133*, 411.

(30) (a) Jortner, J.; Bixon, M. J. *Chem. Phys.* **1988**, *88*, 167. (b) Kestner, N. R.; Logan, L.; Jortner, J. *J. Phys. Chem.* **1974**, *78*, 2148. (c) Efrima, S.; Bixon, M. *Chem. Phys.* **1976**, *13*, 447. (d) Ulstrup, J.; Jortner, J. *J. Chem. Phys.* **1975**, *63*, 4358. (e) Freed, K. M.; Jortner, J. *J. Chem. Phys.* **1970**, *52*, 6272. (f) Meyer, T. J. *Acc. Chem. Res.* **1978**, *11*, 94. (g) Ovchinnikov, A. A.; Ovchinnikov, M. Y. *Adv. Quantum Chem.* **1982**, *16*, 161.

Condon factors using the Golden Rule, has been shown to be important for reactions that are strongly exothermic (e.g., in the Marcus inverted region).[31] For the molecules discussed in the present study, the reaction exothermicity is small ($\Delta G_0 \sim 10$ kcal/mol).[32] The reaction is not in the Marcus inverted region and, thus, these types of quantum mechanical effects are expected to be small.

In this paper, we examine the intramolecular charge-transfer reaction of a series of symmetric and asymmetric alkylated (aminophenyl)sulfones (the general structure is given in Figure 1). We combine information from static and time-resolved spectroscopies and semiempirical calculations and analytic theory to try to determine the nature of the reaction coordinate for the excited-state electron transfer.

Experimental Section

The details of the picosecond emission spectrometer have been previously discussed.[33] Bis(4-aminophenyl)sulfone (APS, Aldrich) was purified by recrystallization from ethanol. The alkylated derivatives were synthesized by refluxing APS with the appropriate trialkyl phosphate in diglyme for at least 15 h.[34] DMAPS was recrystallized from pyridine and dioxane. DEAPS, DPAPS, and DBAPS were purified by silica gel column chromatography using an *n*-hexane/ethyl acetate (7/3 by volume) mixture as the elutant. The [(trialkylamino)phenyl]sulfones, 3-RAPS (R = alkyl group), were also collected from the column. All compounds were characterized by ^{1}H NMR spectroscopy. All solvents were spectral grade (Aldrich), dried over molecular sieves, and checked for background emission.

MNDO Calculations

The ground-state charge distributions of DMAPS was determined by using the AMPAC computer program developed by Dewar and co-workers.[35,36] The calculations used the MNDO all-valence electron parameterization of the NNDO SCF approximation. The results are given in Figure 1. From this calculation, the ground-state dipole moment of DMAPS is calculated to be 9.5 D. Increasing the alkyl chain length (DEAPS, DPAPS, and DBAPS) results in a slightly smaller ground-state dipole moment; see Table I.

In addition to the ground-state electronic structure, calculations were carried out as a function of the angle between the dialkylaminophenyl group and the remainder of the molecule. This rotation is thought to be that involved in separating the charge in the excited state.[32] The shape of the ground-state potential energy surface along this coordinate gives information on those excited-state geometries that can be accessed by direct electronic excitation. The minimum energy was found for a dihedral angle of 0° and 180°, as expected. The energy barrier to rotation (with the twisted geometry at $\theta = 90°$ being the transition state) is 3.2 kcal/mol. These calculations are for the isolated molecule in the absence of dielectric interactions with the solvent. As twisting on the ground-state potential surface induces a separation of charge in the molecule, polar solvents will stabilize this motion. Thus, the above calculations provide an upper bound for the energy barrier and a lower bound for the range of dihedral angles populated at room temperature. From these calculations, the distribution of molecules as a function of the torsion angle can be calculated. The potential was fit to a quadratic function and, assuming a Gaussian distribution of molecules, 67% of the ground state population exhibit dihedral angles 0 ± 10°.

Steady-State Absorption and Emission Spectroscopy

The steady-state emission spectra of DMAPS in *n*-butyl chloride and methanol are shown in Figure 2. In *n*-butyl chloride, emission from the LE state dominates the spectrum. In alcohols, two

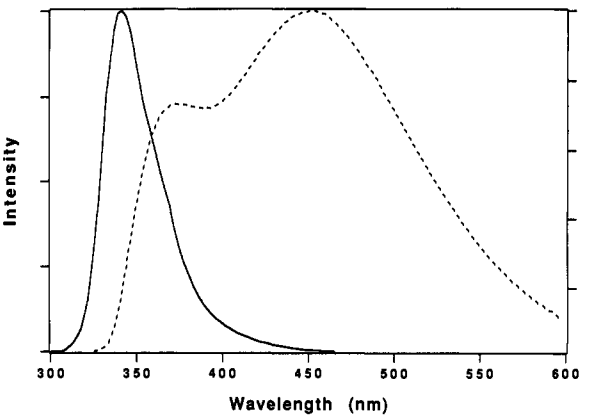

Figure 2. Steady-state emission spectrum of DMAPS in room temperature *n*-butyl chloride (—) and methanol (- - -) solutions.

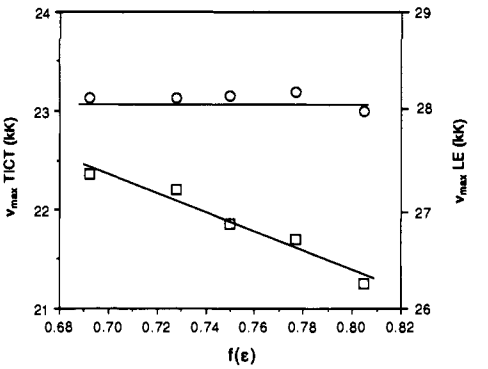

Figure 3. Emission maximum of the LE (○) and TICT (□) bands of DEAPS plotted as a function of the dielectric properties of the solvent; $f(\epsilon)$ is defined in eq 2. The weak dependence of the emission maximum of the LE band indicates that the dipole moment changes only slightly upon excitation to this state. The sensitivity of the TICT emission indicates a large increase in the dipole moment. With a cavity radius of 3.7 Å, the TICT dipole moment is estimated to be ~18 D (see Table I).

overlapping emission bands are observed. The position of the LE emission is slightly red-shifted from that observed in *n*-butyl chloride. In addition, a broad structureless emission is observed in the visible region. This has previously been assigned to emission from the TICT state.[32] Studies in polar aprotic solvents indicate that the red-shifted emission is not a result of a specific hydrogen-bonding interaction between the solvent and the chromophore.[32] The maximum of the emission from the twisted intramolecular charge transfer (TICT) state is dependent on solvent. Bluer emission bands are observed with decreasing solvent polarity. Similar results are observed for all the sulfones. These data reveal that the static Stokes shift ($\nu_a - \nu_f$) is solvent dependent. Within a dielectric continuum description of the solvent, the Stokes shift can be expressed in terms of the Lippert–Mataga equation.[37]

$$\nu_a - \nu_f = \frac{2}{hc}\left[\frac{\epsilon - 1}{2\epsilon + 1} - \frac{n^2 - 1}{2n^2 + 1}\right]\frac{(\mu_{es}^2 - \mu_{gs}^2)}{a^3} = \frac{2}{hc}\frac{(\mu_{es}^2 - \mu_{gs}^2)}{a^3} f(\epsilon) \quad (2)$$

In eq 2, h is Plank's constant, c is the speed of light, ϵ is the static dielectric constant, n is the index of refraction, and a is the radius of the spherical molecular cavity.

In order to determine the emission maxima of the LE and TICT bands, the spectra were deconvoluted by using procedures that have been commonly used to study dual emissive molecules.[38] The

(31) (a) Closs, G. L.; Miller, J. R. *Science* **1988**, *240*, 440. (b) Gould, I. R.; Moser, J. E.; Armitage, B.; Faris, S. *J. Am. Chem. Soc.* **1989**, *111*, 1917. (c) Chen, P.; Duesing, R.; Graff, D. K.; Meyer, T. J. *J. Phys. Chem.* **1991**, *95*, 5850.
(32) Rettig, W.; Chandross, E. A. *J. Amer. Chem. Soc.* **1986**, *107*, 5617.
(33) Simon, J. D.; Su, S.-G. *J. Chem. Phys.* **1987**, *87*, 7016.
(34) Heymann, H.; Fieser, L. F. *J. Am. Chem. Soc.* **1945**, *67*, 1979.
(35) Program from Quantum Chemistry Program Exchange. Indiana University Chemistry Department, QCPE Number 506, 1985.
(36) (a) Dewar, M. S. J.; Thiel, W. *J. Am. Chem. Soc.* **1977**, *99*, 4899. (b) Dewar, M. S. J.; Thiel, W. *J. Am. Chem. Soc.* **1977**, *99*, 4907.
(37) See: Lakowicz, J. R. *Principles of Fluorescence Spectroscopy*; Plenum: New York, 1983.
(38) (a) Rettig, W. *Angew. Chem., Int. Ed. Engl.* **1986**, *25*, 971. (b) Lippert, E.; Rettig, W.; Bonacic-Koutecky, V.; Heisel, F.; Miehe, J. A. *Adv. Chem. Phys.* **1987**, *68*, 1.

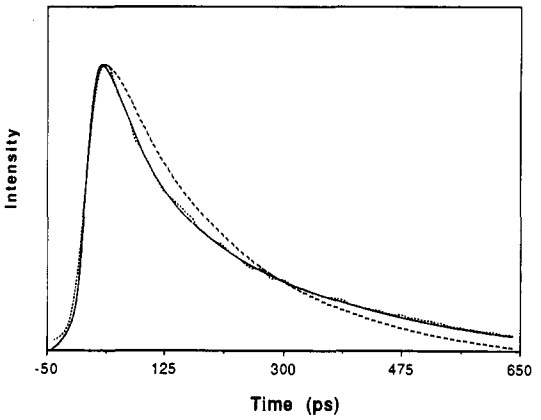

Figure 4. Time dependence of the LE emission from DMAPS in butanol at −30 °C is shown (···). The calculated curves are the best single-exponential fit (---) and multiexponential fit (—) to the data. From the multiexponential fit, the first and second moments of the population decay are 185 (±25) ps and 276 (±40) ps, respectively.

deconvoluted spectra demonstrate that, for wavelengths shorter than 360 nm, only LE emission is observed.

Using the maxima obtained from the deconvolved spectra, eq 2 can be used to estimate μ_{LE} and μ_{CT}. Relevant data for DEAPS are shown in Figure 3. In the series of alcohol solvents, the LE state emission exhibits essentially no dependence on solvent polarity. The TICT state emission, on the other hand, shows a strong dependence. Using a molecular volume[39] of 225 Å^3, the slopes of the least-squares lines shown in Figure 3 reveal a difference of ~1 and 10 D between the ground state and the LE and TICT excited states, respectively. Combined with the MNDO value of the ground-state dipole moment, the TICT state is characterized by a dipole moment on the order of 20 D. This result is consistent with the TICT state involving a full charge separation between the two halves of the molecule.

Time-Resolved Measurements

As stated above, the emission decay for $\lambda \leq 360$ reveal only the population decay of the LE state. Time-resolved narrow band emission (1-nm FWHM) data indicate that the emission dynamics are invariant over the region from 330 to 360 nm.

In quantifying the population decay, the emission data were fit to eq 3. In the eq 3, A_i and τ_i are the amplitudes and time

$$I(t,\lambda) = \int_{-\infty}^{t} [\sum_i A_i e^{(t-\tau)/\tau_i}] G(\tau)\, d\tau \qquad (3)$$

constants for a multicomponent fit to the data. $G(\tau)$ is the instrument response. In general, three exponentials were required to fit the population decay. As an example, in Figure 4, the best fit of a single-exponential and triple-exponential function are compared to experimental data obtained for DMAPS in butanol at −30 °C. The early time dynamics require using a triple-exponential function to accurately reproduce the experimental data.

To characterize the nonexponentiality of the fluorescence decays, the first two moments, τ_a and τ_b, defined by eqs 4 and 5, respectively, were determined.

$$\tau_a = \sum_{i=1}^{n} A_i \tau_i \qquad (4)$$

$$\tau_b = \frac{1}{\tau_a} \sum_{i=1}^{n} A_i \tau_i^2 \qquad (5)$$

The values of τ_a and τ_b for several of the molecules studied are given in Tables II–IV. It is important to note that the values of τ_a and τ_b are essentially insensitive to changes in the size of the rotating dialkylanilino group. In addition, the population decays are also fairly insensitive to the symmetry of the molecule (compare DPAPS and 3-PAPS). For a single-exponential decay, one would expect τ_a to be equal to τ_b. The differences between the two moments indicate the extent of nonexponentiality in the population decays. With decreasing temperature, the values of τ_a and τ_b converge. Thus, while the value of τ_a/τ_b is insensitive to the size of the dialkylanilino group, the deviations from exponential behavior are solvent and temperature dependent.

(39) (a) Edward, J. T. *J. Chem. Ed.* **1970**, *47*, 261. (b) Bondi, A. *J. Phys. Chem.* **1964**, *68*, 411.

Table II. First and Second Moments of the Emission Decays at 340 nm for DPAPS in the Linear Alcohol Solutions as a Function of Temperature

	τ_a, τ_b,[a] ps					
T, °C	methanol	ethanol	propanol	butanol	pentanol	hexanol
22	19[b]	24[b]	32, 42	43, 66	60, 106	85, 114
1	21[b]	26, 42	46, 80	67, 119	112, 178	170, 257
−11	23[b]	31, 50	64, 122	124, 178	164, 254	260, 361
−21	25[b]	45, 62	91, 161	165, 236	216, 318	329, 441
−44	27, 45	77, 174	236, 327	278, 399	418, 561	572, 639
−59	45, 89	153, 260	336, 467	424, 556	556, 668	673, 719
−69	61, 111	184, 300	402, 546	547, 639	731, 769	702, 715

[a] Error in the determination of τ_a and τ_b is ≈±15%. [b] Population decays are well described by a single exponential $\tau_a = \tau_b$.

Table III. First and Second Moments of the Emission Decays at 340 nm for DBAPS in the Linear Alcohol Solutions as a Function of Temperature

	τ_a, τ_b,[a] ps					
T, °C	methanol	ethanol	propanol	butanol	pentanol	hexanol
22	17[b]	22[b]	31, 52	58, 90	62, 106	91, 134
1	20, 30	35, 58	49, 95	93, 148	108, 174	154, 245
−11	25, 41	46, 90	65, 139	144, 214	171, 258	219, 360
−21	26, 42	52, 107	91, 179	169, 270	199, 329	354, 442
−44	32, 65	91, 177	214, 316	298, 418	454, 550	559, 668
−59	59, 103	157, 256	336, 458	476, 558	616, 695	617, 684
−69	64, 118	215, 340	428, 565	572, 663	754, 772	647, 710

[a] Error in the determination of τ_a and τ_b is ≈±15%. [b] Population decays are well described by a single exponential $\tau_a = \tau_b$.

Table IV. First and Second Moments of the Emission Decays at 340 nm for 3-PAPS in the Linear Alcohol Solutions as a Function of Temperature

	τ_a, τ_b,[a] ps					
T, °C	methanol	ethanol	propanol	butanol	pentanol	hexanol
22	20[b]	28, 40	44, 60	67, 104	89, 156	129, 219
1	23[b]	34, 47	64, 112	108, 172	133, 235	197, 324
−11	24[b]	44, 68	94, 151	149, 240	205, 330	321, 438
−21	27, 33	62, 95	120, 199	200, 287	278, 400	387, 509
−44	33, 48	122, 202	252, 378	386, 500	484, 602	692, 765
−59	49, 89	164, 268	380, 539	522, 646	698, 768	746, 762
−69	63, 116	244, 374	464, 623	661, 786	799, 829	781, 810

[a] Error in the determination of τ_a and τ_b is ≈±15%. [b] Population decays are well described by a single exponential $\tau_a = \tau_b$.

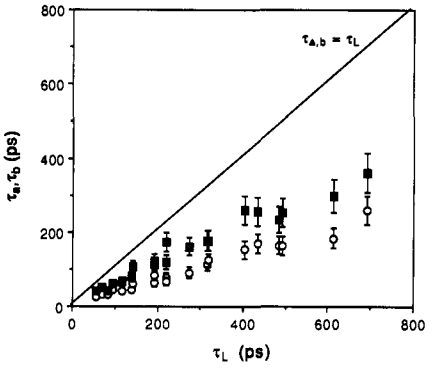

Figure 5. First two moments of the population decay of the LE state of DPAPS, τ_a (○) and τ_b (■), are plotted as a function of the longitudinal relaxation time of the solvent, τ_L. The complete set of data is given in Table II. The data exhibited in this figure were restricted to values of τ_L less than 800 ps.

In Figure 5, τ_a and τ_b are plotted as a function of τ_L for DPAPS in alcohol solutions at various temperatures. The complete set of data is given in Table II; the plot was restricted to τ_L values less than 800 ps. For all cases studied, both moments are faster than the solvation time, τ_L.

Comparisons with Theoretical Models

The above discussion of the static spectroscopy indicates that the dynamics of the emission in the LE band are a measure of the intramolecular electron-transfer process. In comparing the experimental data to theoretical models, the following observations need to be accounted for: (1) the population decay is nonexponential, (2) the first moment, τ_a, for the entire series of DRAPS molecules studied is substantially faster than both τ_L and the average solvation times determined from $C(t)$ measurements in the long-chain alcohols (propanol–hexanol) and low-temperature methanol and ethanol solution, and (3) the values of τ_a and τ_b are invariant with the size of the dialkylamino group.

1. Insights from the Effect of Molecular Size. In dealing with molecules that undergo twisted intramolecular charge transfer, the coupling of the geometry change to the electron-transfer process is generally not known. In the DRAPS series, the charge transfer is thought to involve rotation about the anilino–sulfur bond. This rotation of the substituted aromatic group involves displacement of nearby solvent molecules. Barbara and co-workers[40] have demonstrated that solvent viscosity effects can be observed on rotating groups as small as a $C(CH_3)_2$. Therefore, one would expect that the rotational dynamics of (dimethylamino)phenyl and (dibutylamino)phenyl groups would be substantially different. If significant rotational motion were required for the charge transfer to occur, smaller reaction rate constants should be observed with increasing alkyl substitution of the amino group.

The insensitivity of the electron-transfer dynamics to the size of the dialkylamino group supports a conclusion that the degree of twisting required for populating the TICT state from the LE state is small. Although no theoretical models of the twisting coordinate of DRAPS have been reported, calculations on the excited-state electron transfer of DMABN in polar solvents support a similar conclusion.[41,42] In particular, Schenter and Duke[42] have found that the excited-state reaction in this molecule involves motion in the torsional coordinate (the rotation of the dialkylamino group with respect to the aromatic plane) followed by solvent relaxation. Assuming a planar ground-state geometry, results from gas-phase spectroscopy and CNDO calculations of photoionization spectra show that the equilibrium geometry of the LE state and the crossing from the LE to CT state at constant solvent polarization occur at a twist angle of 30° and 70°, respectively.[43] Thus, a rotation of the dialkylamino group to the perpendicular geometry is not required to enable the charge transfer to occur. Only a small motion, ~40° is needed from the LE equilibrium geometry. These calculations would suggest that viscosity effects on the formation of the TICT state of DMABN would be negligible. This has been experimentally verified by Eisenthal and co-workers.[28] The calculations of Schenter and Duke[42] were also able to quantitative account for the time-resolved emission data for DMABN in alcohols reported by Su and Simon[17e] and Heisel and Meihe.[44]

In light of the above observations, in the DRAPS series, one could envision that in one limit, the reaction dynamics can be controlled by small fluctuations in the torsion angles between the donor and acceptor group (or other relevant vibrational modes). On the other hand, the insensitivity of the rate constant to the size of the rotating group could indicate a solvent-controlled reaction. In the remainder of this discussion, we examine the dynamic data in terms of theoretical models that address these possibilities.

2. One-Dimensional Solvent Coordinate Models. Barbara and co-workers have recently developed a semiempirical model for excited-state intramolecular electron-transfer reactions.[26] In their approach, the reaction occurs on an adiabatic free energy surface; the reaction coordinate involves only solvent dielectric relaxation. The calculated adiabatic surface enables one to predict the steady-state absorption and emission spectra. In addition, time-dependent spectra can be generated by assuming an equation of motion (i.e., Langevin or Smoluchowski) for the population on the reaction surface and position dependent radiative and nonradiative rate constants. Barbara and co-workers have successfully used this approach to quantitatively model the static and time-resolved spectra of ADMA and BA in several polar aprotic solvents. In an attempt to determine whether or not the reaction process of DRAPS is controlled by solvent dielectric relaxation, this model was used to calculate steady-state emission spectra.

In order to calculate the adiabatic reaction surface, one begins by assuming that the diabatic ground, LE, and CT states are harmonic in the solvent coordinate, x, with the same force constant, k_s. While the energy separation between the ground state and the electronically excited LE and CT states is large, the LE and CT states are close in energy. Thus, it is reasonable to conclude that the excited states of the molecule, Ψ_{es}, are more accurately described by a linear combination of the two diabatic states, Ψ_{LE} and Ψ_{CT}.

$$|\Psi_{es}(\mathbf{x})\rangle = c_1(\mathbf{x})|\Psi_{LE}\rangle + c_2(\mathbf{x})|\Psi_{CT}\rangle \tag{6}$$

The coefficients, $c_1(\mathbf{x})$ and $c_2(\mathbf{x})$ determine the relative contributions of the diabatic LE and CT states to the excited-state wave function for a particular value of the solvent coordinate, x, and are determined by diagonalizing the 2 × 2 Hamiltonian matrix. This requires knowledge of the solvent-independent electronic coupling matrix element, H_{in}, between the LE and CT states. Unfortunately, there is no current method for measuring this value. In using this model, the interaction matrix element is varied in order to minimize the deviations between the experimental and simulated spectra.

Diagonalization of the Hamiltonian generates the adiabatic excited-state surfaces. These are then used to generate steady-state emission spectra. The intensity of the fluorescence spectrum as a function of frequency is calculated by evaluating the transition moment integral:

$$I(\nu) = \int_{-\infty}^{\infty} d\mathbf{x}\, |M(\mathbf{x})|^2 \rho(\mathbf{x}) \tag{7}$$

where $|M(\mathbf{x})|^2$ is the square of the transition moment and $\rho(\mathbf{x})$ is the population distribution function. It is common to separate the transition moment into electronic and vibrational components. The electronic contribution can be estimated from the radiative rate constants obtained in polar and nonpolar solvents. In nonpolar solvents, only emission from the LE state is observed. Comparison of the spectra in polar and nonpolar solvents provides the magnitude of the relative transition moments of the LE and CT states. For alcohol solvents, this ratio is ~0.3. The vibrational part of the transition moment is more difficult to calculate. It requires knowledge of the Franck–Condon factors associated with the different vibrations of the molecule. Barbara and co-workers evaluated this part of the transition moment by measuring the emission line shape in a nonpolar solvent. As the transition strength is predominantly derived from the contribution of the diabatic LE state to the total wave function, the line shape of the molecule in polar solvent is assumed to be identical with that of the pure LE state observed in the nonpolar solvent. With the assumption that the line shape is independent of x, the spectra can be computed once the distribution function, $\rho(\mathbf{x})$, is specified. As used previously by Tominaga et al.,[26] $\rho(\mathbf{x})$ is assumed to be Boltzmann.

(40) Flom, S. R.; Nagarajan, V.; Barbara, P. F. *J. Phys. Chem.* **1986**, *90*, 2085.
(41) (a) Rettig, W.; Bonacic-Koutecky, V. *Chem. Phys. Lett.* **1979**, *62*, 115. (b) Leinhos, U.; Kuhnle, W.; Zachariasse, K. A. *J. Phys. Chem.* **1991**, *95*, 2013. (c) Weisenborn, P. C. M.; Huizer, A. H.; Varma, C. A. G. O. *Chem. Phys.* **1989**, *133*, 437. (d) LaFemina, J. P.; Duke, C. B.; Paton, A. *J. Chem. Phys.* **1987**, *87*, 2151.
(42) Schenter, G. K.; Duke, C. B. *Chem. Phys. Lett.* **1991**, *176*, 563.
(43) (a) Warren, J. A.; Bernstein, E. R.; Seeman, J. I. *J. Chem. Phys.* **1988**, *88*, 871. (b) Grassian, V. H.; Warren, J. A.; Bernstein, E. R.; Secor, H. V. *J. Chem. Phys.* **1989**, *90*, 3994.
(44) (a) Heisel, F.; Miehe, J. A. *Chem. Phys. Lett.* **1985**, *98*, 233. (b) Heisel, F.; Miehe, J. A. *Chem. Phys. Lett.* **1985**, *98*, 243.

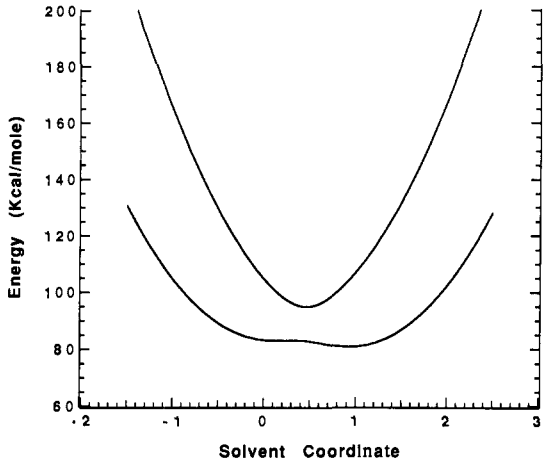

Figure 6. Calculated potential energy curves for the excited states of DMAPS from the semiempirical solvent coordinate model of Barbara and co-workers. These curves resulted from minimizing the deviations between calculated and experimental spectra (shown in Figure 7). The three parameters varied were the exothermicity ($\Delta G°$), the force constant (k_s, assumed to be the same for all states), and the mixing matrix element between the LE and TICT states, H_{int}. The values for $\Delta G°$, k_s, and H_{int} for the surfaces shown are 2.6, 41, and 6 kcal/mol, respectively.

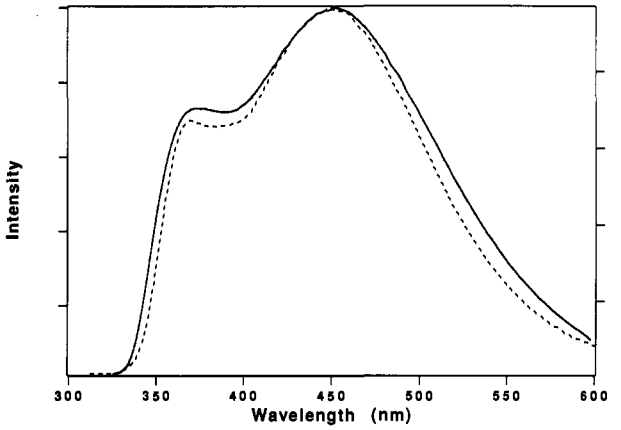

Figure 7. Experimental emission spectrum (—) of DMAPS in methanol at 0 °C are compared to calculations (---) by using the potential energy surfaces shown in Figure 6. The theoretical model is not able to reproduce the experimental spectra. These calculations are unable to accurately represent the line width of the TICT emission and underestimate the emission in the region between the maxima of the LE and TICT bands.

In Figure 6, the calculated adiabatic surfaces are shown for DMAPS in methanol. $\Delta G°$, k_s, and H_{int} were varied to give the best agreement between the calculated and experimental spectra. In Figure 7, calculated emission spectra are compared with experimental data for methanol. These results represent the best fits that could be obtained from the above-described formalism. The values for $\Delta G°$, k_s, and H_{int} used to calculate the spectra shown in Figure 7 are 2.6, 41, and 6 kcal/mol, respectively. While the agreement between experiment and calculation appears acceptable, the parameters obtained merit closer examination.

It is experimentally possible to estimate the solvent force constant from the time-dependent Stokes shifts of emitting polar probe molecules. The CT emission from DMAPS exhibits such a time-dependent emission spectrum, giving solvation times similar to that observed for many Coumarin probe molecules.[13] If we assume that the force constants of the CT and ground state are the same and that the potential is harmonic, the magnitude of the Stokes shift can be used to determine the force constant. This approach gives a solvent force constant on the order of 10 kcal/mol, a factor of 4 smaller than the value obtained from the application of the model of Barbara and co-workers. One could question the assumption that the solvent force constant, k_s, is the same for the CT and ground states. The dependence of the solvent force constant on the molecular charge distribution has been addressed in many recent theoretical discussions. Kakitani and Mataga (KM)[45] have suggested that this value can vary significantly with changing solute properties. On the other hand, King and Warshel[46] have reported that the predictions of the KM theory overestimate the effect and that the force constant remains fairly constant over a wide range of solute charge distributions. This later conclusion is consistent with recent molecular dynamics simulations.[20-24] In the absence of fast solvation effects, these studies support the conclusion that value of k_s obtained in the application of the model of Barbara and co-workers is inconsistent with experimental observations.

The magnitude of the coupling matrix element, H_{int}, also deserves further discussion. As mentioned above, there is no accepted method for experimentally measuring H_{int}. However, a value of 6 kcal/mol appears to be inconsistent with values reported for similar organic intramolecular charge-transfer systems. In detailed studies of BA and ADMA, Barbara and co-worker reported values of ~1 kcal/mol. In both of these cases this magnitude of the coupling matrix element was considered to be large. If one assumes that the oscillator strength of the CT state results from mixing with the LE state, the time dependence of the total emission intensity suggests that the coupling is weaker in DRAPS than in either ADMA or BA, in contrast to values obtained by using this model.

The above analysis suggests that the reaction is not completely described by a model that restricts the reaction coordinate to involving only solvent motion. While the observed emission spectra can be fit by the calculated spectra, the parameters used do not seem to reflect the system in general. Therefore, we now examine theoretical models that include both solvation and the effects of the vibrational degrees of freedom in the reacting molecule.

3. Two-Dimensional Reaction Models. The importance of vibrational motion in adiabatic electron-transfer reactions has recieved considerable attention. For example, for the Fe$(H_2O)^{3+}$/Fe$(H_2O)^{2+}$ exchange reaction, the total reorganization energy is predicted to be ~2.6 eV, with 1.5 eV originating from the inner-sphere contributions associated with changes in bond lengths and bond force constants in going from reactant to product.[48] In this section we examine a theoretical model developed by Sumi, Nalder, and Marcus (SNM), which takes into account contributions to the reaction rate constant from both fluctuations in the vibrational (or torsional) coordinates and solvent motion.[6]

In the SNM treatment, the reaction dynamics are modeled by using a modified Smoluchowski diffusion equation. Motion along the solvent coordinate is controlled by dielectric relaxation. Treating the solvent as a dielectric continuum, the relevant time scale is τ_L. The solvent-coordinate-dependent reaction rate constant, $k(\mathbf{x})$, depends on solvation through the activation energy and vibrational contributions through the prefactor. Comparing the kinetic data to predictions based on the SNM model provides a measure of the ratio of the inner- and outer-sphere contributions, λ_i/λ_0, to the total reorganization energy, λ.

In the SNM treatment, the diffusion equation is used to calculate a probability distribution function $P(\mathbf{x},t)$ from which the survival probability, $Q(t)$, is obtained.

$$Q(t) = \int_{-\infty}^{\infty} d\mathbf{x}\, P(\mathbf{x},t) \qquad (8)$$

In connecting to experimental measurements, the theoretical quantity $Q(t)$ is equivalent to the experimentally determined

(45) (a) Kakitani, T.; Mataga, N. *J. Phys. Chem.* **1985**, *89*, 4752. (b) Kakitani, T.; Mataga, N. *J. Phys. Chem.* **1986**, *90*, 993. (c) Hatano, Y.; Saito, M.; Kakitani, T.; Mataga, N. *J. Phys. Chem.* **1988**, *92*, 1008. (d) Yoshimori, A.; Kakitani, T.; Mataga, N. *J. Phys. Chem.* **1989**, *93*, 3694. (e) Yoshimori, A.; Kakitani, T.; Enomoto, Y.; Mataga, N. *J. Phys. Chem.* **1989**, *93*, 8316.
(46) King, G.; Warshel, A. *J. Chem. Phys.* **1990**, *93*, 8682.
(47) Kim, H. J.; Hynes, J. T. *J. Phys. Chem.* **1990**, *94*, 2736.
(48) (a) Sutin, N. In *Tunneling in Biological Systems*; Chance, B., de Vault, D. C., Frauenfelder, H., Marcus, R. A., Schrieffer, J. R., Sutin, N., Eds.; Academic Press: New York, 1979; p 201. (b) Gratzel, M. *Heterogeneous Photochemical Electron Transfer*; CRC Press: Boca Raton, FL, 1989.

Table V. Values for k_e at −20 °C for the Various Sulfone Molecules Studied[a]

solvent	DMAPS	DEAPS	DPAPS	DBAPS	3-PAPS	3-BAPS	⟨DRAPS⟩
MeOH	4.2	4.0	5.9	4.7	4.0	4.3	4.5
EtOH	2.0	2.2	2.7	3.2	2.3	1.9	2.4
ProOH	1.6	1.5	2.2	2.6	1.5	1.1	1.8
ButOH	1.3	1.3	0.89	1.3	1.0	0.98	1.1
PentOH	0.84	0.97	0.86	0.84	0.81	0.82	0.86
HexOH	0.57	0.50	0.42	0.44	0.44	0.41	0.46

[a] These values were determined by using the population decays of the LE state as described in the text. (Rate constants are in units of 10^{10} s^{-1}, errors in rate constants are ±15%). The final column is the average value of k_e from the data for the entire series of alkylated derivatives studied.

Table VI. Activation Energies (kcal/mol) Determined from the Temperature Dependence of k_e for the Various Sulfones

solvent	DMAPS	DEAPS	DPAPS	DBAPS	3-PAPS	3-BAPS
MeOH	0.8 ± 0.1	0.8 ± 0.1	0.8 ± 0.1	1.2 ± 0.1	0.8 ± 0.1	0.7 ± 0.1
EtOH	2.9 ± 0.1	3.5 ± 0.6	2.9 ± 0.3	2.1 ± 0.2	2.9 ± 0.1	2.7 ± 0.1
ProOH	3.1 ± 0.8	3.7 ± 0.6	3.2 ± 0.4	3.8 ± 0.6	2.2 ± 0.2	2.6 ± 0.2
ButOH	4.1 ± 0.7	3.2 ± 0.4	2.9 ± 0.5	3.2 ± 0.3	3.1 ± 0.3	2.6 ± 0.1
PentOH	3.8 ± 0.4	3.9 ± 0.6	3.4 ± 0.4	4.5 ± 0.8	3.8 ± 0.4	2.8 ± 0.1
HexOH	3.3 ± 0.3	3.6 ± 0.4	3.3 ± 0.4	3.6 ± 1.0	3.6 ± 0.8	2.5 ± 0.3

Table VII. Activation Energies (kcal/mol) for DBAPS in the Alcohols Determined from the Temperature Dependence of k_e, τ_a, and τ_b

	MeOH	EtOH	ProOH	ButOH	PentOH	HexOH
k_e	1.2 ± 0.1	2.1 ± 0.2	3.8 ± 0.6	3.2 ± 0.3	4.5 ± 0.8	3.6 ± 1.0
τ_a	1.8 ± 0.3	3.0 ± 0.6	3.6 ± 0.8	3.0 ± 0.6	3.2 ± 0.6	2.6 ± 0.4
τ_b	2.4 ± 0.4	3.2 ± 0.7	3.0 ± 0.6	2.5 ± 0.4	2.6 ± 0.4	2.1 ± 0.3

population decay of the LE state. In the limit of a barrierless solvent-controlled reaction, the population decay is predicted to follow an exponential decay with time constant τ_L.[49] This is identical with the results predicted by many current theories.[7,8,13,29] The majority of the experimental data obtained on the DRAPS molecules reveal nonexponential population decays that are characterized by average survival probabilities and that are significantly less than τ_L. Thus, within a continuum description of the solvent, these observations suggest that the reaction is not solvent controlled, in agreement with conclusions obtained in the previous section. As we are interested in probing the potential role of vibrational modes in determining the reaction dynamics, the following discussion is restricted to the limit of the SNM theory where such contributions are important. In this case, the thermally equilibrated reaction rate constant, k_e, and the survival probabilty, $Q(t)$, can be evaluated by using eqs 9 and 10. In eqs 9 and 10,

$$k_e = \langle k(\mathbf{x})\rangle_0 = \int_{-\infty}^{\infty} d\mathbf{x}\ k(\mathbf{x}) P_0(\mathbf{x}) \tag{9}$$

$$Q(t) = \int_{-\infty}^{\infty} d\mathbf{x}\ P_0(\mathbf{x}) e^{-k(\mathbf{x})t} \tag{10}$$

P_0 is the equilibrium probability distribution at time zero. In other words, the solvent polarization at $t = 0$ is assumed not to evolve on the time scale of the reaction. In this limit, eqs 9 and 10 enable k_e to be directly related to $Q(t)$, as shown below.

$$k_e = -\frac{d}{dt} Q(t)|_{t=0} \tag{11}$$

In analyzing the data, $Q(t)$ is fit to a series of exponentials. Thus in terms of the time constants, τ_i, and corresponding prefactors, A_i, the equilibrated reaction rate k_e is given by

$$k_e = \sum_{i=1}^{n} A_i/\tau_i \tag{12}$$

Table V gives the values of k_e at −20 °C for the molecules in the various alcohols studied. These data show that the rate constant is essentially identical for the various alkylated derivatives. From these values, the activation energies can be determined. In Figure 8, ln (k_e) is plotted as a function of the inverse of the solution temperature for DPAPS in butanol. This plot reveals the expected linear dependence. Similar plots were obtained for all the molecules and solvents studied. The various activation energies determined in this manner are given in Table VI. The data in Table VI suggest that the barrier to reaction in methanol is less than that observed in the other solvents. However, it is likely that this is due to the limited time resolution of the experiments. As k_e is weighted toward the early time dynamics of the population decays, such effects will become more pronounced in the shorter chain alcohol solvents. To test this possibility, barriers were also determined from the temperature dependence of τ_a and τ_b. It is expected that these data will be less sensitive to the possible fast components of the population decays. In Table VII the values for DBAPS are given. These data show that for the longer chain alcohols (propanol to hexanol), the barriers determined from the survival times are within experimental error of those obtained from the temperature dependence of k_e. However, in methanol and ethanol, the activation energies determined from τ_a and τ_b are higher than that found for k_e but similar to those found for the longer chain alcohols. This suggests that the reaction barrier is essentially constant over the range of solvents studied.

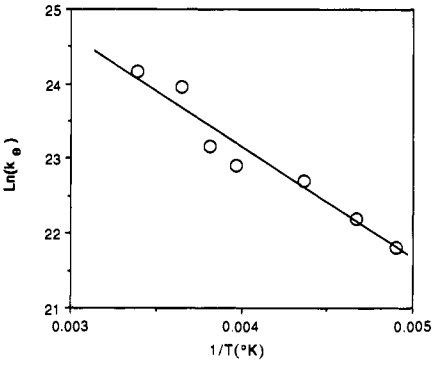

Figure 8. The log of the thermally equilibrated reaction rate constant, ln (k_e), is plotted as a function of the inverse temperature for the intramolecular charge-transfer reaction of DPAPS in butanol. The slope of the least-squares fitted line indicates an activation energy of 2.9 kcal/mol.

In determining the ratio of λ_i/λ_0, the SNM treatment examines the dependence of log ($k_e\tau_a$) on $\log_{10}$ ($k_e\tau_L$) at constant ΔG^*. In Figure 9, log ($k_e\tau_a$) is plotted as a function of log ($k_e\tau_L$) for DMAPS, DBAPS, and 3-BAPS in the series of alcohols over the

(49) Alcohols are generally characterized by three regions of Debye dispersion. In calculating the τ_L values used to quantify the comparison with the SNM model, the longest Debye relaxation time (associated with the making and breaking of hydrogen bonds) is used.

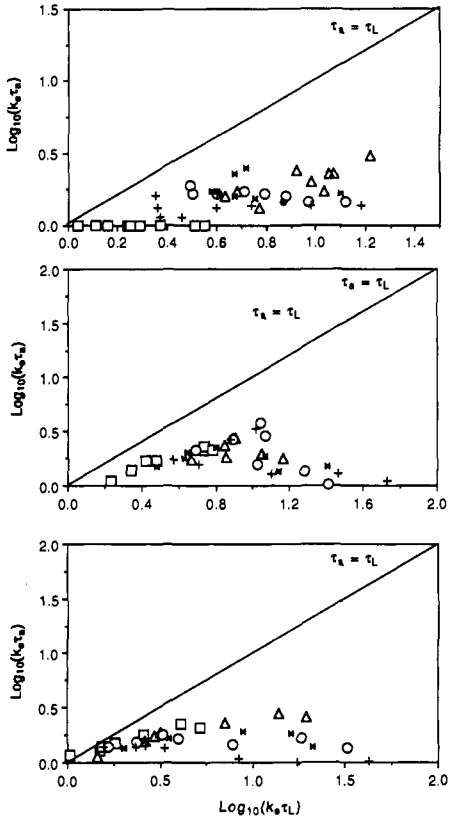

Figure 9. log ($k_e\tau_a$) is plotted as a function of log ($k_e\tau_L$) for DMAPS (top), DBAPS (middle), and 3-BAPS (bottom) in alcohol solutions at various temperatures. The solid line represents the case where $\tau_a = \tau_L$. The solvents plotted are ethanol (□), propanol (△), butanol (✱), pentanol (○), and hexanol (+). Within each solvent, increasing values of log ($k_e\tau_L$) correlate with decreasing temperature.

temperature range studied. The solid line given in these plots is for $\tau_a = \tau_L$. Comparison with simulated plots of log ($k_e\tau_L$) vs log ($k_e\tau_a$) suggest that the ratio λ_i/λ_0 is greater than 1. These plots also reveal that the behavior of these three molecules is very similar despite their difference in size and symmetry. This comparison between the kinetic data and the SNM theory support a conclusion that fluctuations in the intramolecular coordinates play a significant role in determining the reaction rate constant.

These conclusions, however, are based on several assumptions that are not obviously satisfied by the experimental system. First, the barrier to reaction is assumed to be independent of temperature and solvent (the Nadler–Marcus simulations of log ($k_e\tau_L$) vs log ($k_e\tau_a$) are carried out at constant ΔG^*).[6] Second, as stated at the beginning of our discussion of the SNM model, the time scale for solvent dynamics is gauged by τ_L. The validity of this assumption is controversial and is examined in the last section of this discussion.

The effect of solvent and temperature on the barrier heights of intramolecular charge-transfer reactions was first addressed in detail by Eisenthal and co-workers.[29] In that study, the photoinduced excited-state charge-transfer reaction of DMABN in nitrile solvents was examined. These workers demonstrated that in the series of alkyl nitriles, the activation free energy for charge-transfer reaction changes with solvent polarity. These effects could be quantitatively accounted for by a linear free energy relationship in which the activation energy was parameterized in terms of the empirical solvent polarity variable $E_T(30)$.[50] This model has also been theoretically justified by Sparpaglione and Mukamel.[10] The linear dependence of the activation energy on solvent polarity was shown to result in cases where the reorganization energy is large. We have previously used a similar analysis

(50) Reichardt, C. *Solvents and Solvent Effects in Organic Chemistry*; VCH: Weinheim, 1988.

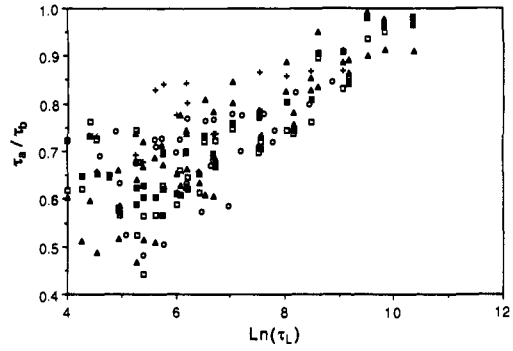

Figure 10. Ratio of the first two moments of the population decay of the LE state, τ_a/τ_b, is plotted as a function of the logarithm of the solvent relaxation time, ln (τ_L). The experimental data for the series of alcohol solvents ethanol to hexanol over the temperature range ~20 to ~−70 °C. The molecules studied are (○) DMAPS, (+) DEAPS, (□) DPAPS, (△) DBAPS, (■) 3-PAPS, and (▲) 3-BAPS. With increasing τ_L, the population decay approaches single-exponential character ($\tau_a = \tau_b$). This observation is accounted for by a combination of changes in the potential energy surface with changing solvent polarity and a narrowing of the population distribution on this surface with decreasing temperature.

on the reaction rates of DRAPS and have found that the reaction barrier is somewhat dependent on solvent polarity.[17g] In the present context, it is instructive to consider the effect of using polarity-corrected reaction rates in generating the plots of log ($k_e\tau_L$) vs log ($k_e\tau_a$). As discussed previously, the approach of Eisenthal and co-workers[28] is difficult to directly apply in the present situation, as the population decays of the LE state are nonexponential.[17g] However, one could obtain some insights by using the average survival time, τ_a, as a measure of the inverse of the average reaction rate constant. Since solvent polarity decreases with increasing alkyl chain length (the $E_T(30)$ values of methanol and hexanol are 55.5 and 50.2, respectively),[50] correcting the rate constants relative to the polarity of methanol, τ_a^{-1} for ethanol through hexanol would increase with respect to the tabulated values. As a result, correction for solvent polarity effects on the reaction barrier would increase the log ($k_e\tau_L$) region probed. Within this approximation, no effect would be observed on the log ($k_e\tau_a$) values. Thus, the polarity-corrected rates would strengthen the above conclusion that $\lambda_i/\lambda_0 > 1$.

Further support for this conclusion is obtained by considering the effect of solvent and temperature on the ratio of the first two moments of the population decay, τ_a/τ_b. In Figure 10, this ratio is plotted for all molecules studied as a function of the logarithm of the solvent relaxation time, ln (τ_L). These data show that with increasing values of τ_L the population decays become more exponential, approaching the limit where $\tau_a = \tau_b$. As $Q(t)$ approaches single-exponential behavior, one might conclude that the dominant contribution to the reaction dynamics changes from fluctuations in the intramolecular modes to solvation dynamics. In the region where $\tau_a \sim \tau_b$, the first moment of the population decay is still approximately 2 orders of magnitude smaller than the characteristic time scale of solvent relaxation. Therefore, it is not reasonable to conclude that the decreasing nonexponentiality of the decay is indicating a dominance of solvent dynamics in controlling the reaction process. The trend observed must be resulting from changes in the potential energy surface.

The trend shown in Figure 10 can be explained within the nondiffusive limit of the SNM theory. In Table VI, the activation energies associated with k_e are tabulated. Within experimental error, these numbers are identical for all molecules studied for the solvents ethanol to hexanol. This is not surprising in light of the above conclusions that the reaction proceeds via intramolecular fluctuations. Within the series of polar alcohols, no effect on such a barrier is expected. However, consider the solvation of the TICT state in the various alcohols. With decreasing polarity (increasing alkyl chain length), the TICT state is destabilized with respect to the LE state. This causes the barrier along the x axis (solvation) to change, while that along the Q axis (vibration) is essentially solvent independent. This is depicted schematically in Figure 11.

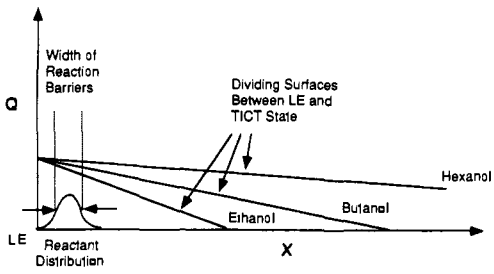

Figure 11. Schematic representation of the changes in the two-dimensional reaction potential with decreasing solvent polarity. Experimentally determined activation barriers indicate that the barrier height along the Q-coordinate is constant in the alcohols ethanol–hexanol. With decrease polarity, the TICT is destabilized relative to the LE state and the crossing point between these two states on the x-coordinate shifts to the right. This serves to "flatten out" the distribution of barriers available to the reacting population, resulting in decay dynamics that approach single-exponential character.

Holding the barrier along the Q-coordinate constant, the net effect of decreased solvent polarity is to change the crossing point between the LE and TICT states along the solvent coordinate. If we consider the equilibrium population of molecules in the reactant well, changes in this crossing point effect the magnitude by which the reaction barrier in the Q-coordinate changes for a given range of the solvent coordinate x. For a fixed width distribution in x, the distribution of barrier heights decreases with decreasing dielectric.

Within this description, for a fixed temperature, the deviation of $Q(t)$ from single-exponential behavior should decrease with increasing alkyl chain length. This is consistent with the experimental data. For example, for DPAPS at −69 °C, the ratio τ_a/τ_b shows such a systematic change: 0.55 (methanol), 0.61 (ethanol), 0.74 (propanol), 0.86 (butanol), 0.95 (pentanol), and 0.98 (hexanol).

Decreasing the temperature in a single solvent results in two competing effects. First, the dielectric constant of the liquid increases, thereby shifting the crossing point of the LE and TICT states along the solvent coordinate, as shown in Figure 11. Second, the distribution of reactant molecules along the solvent coordinate narrows.

For example, between 20 and −34 °C, the dielectric constant of propanol increases from 20 to 29.[50] This stabilizes the TICT state relative to the LE state and moves the intersection point between these surfaces to a larger value in the x-coordinate. In the harmonic SNM model, the width of the distribution in x is given by $2(k_s/2k_BT)^{1/2}$. For this same temperature range, the distribution has narrowed 10% at the lower temperature, thereby sampling a smaller region of the intersecting line between the LE and TICT surfaces. On the basis of the experimental data, the narrowing of the reactant distribution appears to be a larger effect than the increased polarity in determining the nonexponentiality of the decay. In particular, for DPAPS in hexanol, the ratio τ_a/τ_b changes from 0.74 to 0.98 in going from room temperature to −69 °C.

The second reservation on the ability of the SNM theory to account for the experimental data involves the validity of using τ_L to gauge the solvent response. This question is currently the subject of extensive experimental and theoretical work. We now examine several of the current thoughts and their implications on the above conclusions.

4. Implications of Fast Solvation on the Reaction Mechanism. It is clear from Figure 9 that the conclusions drawn from comparison with the SNM model depend on the time scale used to gauge solvent relaxation. The results of this analysis are not affected by using the solvation time, τ_S, determined from $C(t)$ measurements. However, several recent theoretical models suggest that neither τ_L nor τ_S is the correct choice for the relevant solvation time.[11,12] In particular, alcohol solvents are not well characterized by a Debye frequency-dependent dielectric constant.[14] These solvents exhibit a wide range of relaxation times. This is also supported by the nonexponential relaxations observed for $C(t)$ measurements in alcohols. Frequency-dependent models such as those proposed by Hynes[12] strongly support the conclusion that the shorter time solvent dynamics, as opposed to the longer time solvent relaxation (i.e., τ_S), dominate an activated chemical reaction rate. In the case of the present study, these observations would suggest that in alcohol solvents, the slow collective hydrogen bonding dynamics that dominate both dielectric dispersion studies and the average time determined from $C(t)$ are not the major contributions to reaction rates controlled by solvent motion. Such a conclusion is also consistent with models described by Fonseca[11] and several recent molecular dynamic studies[20-24] of charge-transfer reactions. Furthermore, in the case of an adiabatic reaction, polarization diffusion[51-53] (translational solvent motion) effects can contribute to driving the chemical reaction, giving $\tau_a \ll \tau_L$. This limit is expected when the ratio $D_T/2D_R\sigma^2 \geq 0.5$.[54] D_R and D_T are the rotational and translational diffusion coefficients of the solvent molecules, and σ is the hard-sphere diameter of the solute molecule. However, for most alcohol solvents, this ratio is less than unity,[55] suggesting that these components may not dominate the reaction rate. In principle, the time scales of these "fast" motions are reflected by the decay dynamics of $C(t)$. However, recovering the distribution of solvent relaxation times from $C(t)$ measurements and assigning them to particular molecular motions is extremely difficult. $C(t)$ has been determined for several room temperature alcohols and is well described by a biexponential function.[13,18] In general, the fast component comprises about half the response and occurs on a time scale that is about four times faster than τ_S. In addition, recent MD simulations suggest that a large fraction of the $C(t)$ response occurs on a time scale significantly faster than reported experimental resolution.[56-63] Calculations of fast components (~100 fs) have been reported for water, acetonitrile, methanol, and a model polar aprotic solvent. Fleming and co-workers have recently observed experimental evidence of such components using 50-fs time resolution.[18f] If one used these fast solvation times as a measure of the solvation in the SNM model, a plot of log $(k_e\tau_L)$ vs log $(k_e\tau_a)$ would suggest that solvation plays a dominant role, with $\lambda_i/\lambda_0 \ll 1$. Unfortunately, only a small amount of experimental data on fast components in $C(t)$ is available and a quantitative comparison cannot be carried out at present.

In exploring electron-transfer dynamics in non-Debye solvents, Fonseca[11] has demonstrated that reactions can exhibit population decays that are nonexponential and whose time evolution is strongly influenced by the fast solvent relaxation times. These theoretical predictions were also shown to be consistent with stochastic trajectories determined by using the generalized Langevin equation to describe motion along the solvent coordinate.

In light of these comments, at present, it is difficult to use dynamic theories to distinguish between the importance of vibrational fluctuations and fast solvent dynamics in determining charge-transfer reaction rates that are faster than τ_L^{-1}. It is likely

(51) (a) Stiles, P. J.; Hubbard, J. B. *Chem. Phys.* **1984**, *84*, 431. (b) Stiles, P. J.; Hubbard, J. B. *Chem. Phys.* **1985**, *94*, 7.
(52) (a) van der Zwan, G.; Hynes, J. T. *Physica A (Amsterdam)* **1983**, *121A*, 227. (b) van der Zwan, G.; Hynes, J. T. *Chem. Phys. Lett.* **1983**, *101*, 367.
(53) (a) Chandra, A.; Bagchi, B. *Chem. Phys. Lett.* **1988**, *151*, 47. (b) Chandra, A.; Bagchi, B. *J. Phys. Chem.* **1989**, *93*, 6996. (c) Chandra, A.; Bagchi, B. *J. Chem. Phys.* **1990**, *90*, 1832. (d) Chandra, A.; Bagchi, B. *J. Phys. Chem.* **1990**, *94*, 3152.
(54) For example, for 1-propanol at room temperature, $D_T = 0.7 \times 10^{-5}$ cm^2 s^{-1}, $D_R = 1/2\tau_l$ where $\tau_l \sim 100$ ps; $\sigma = 5$ Å; this gives a ratio of 0.28.
(55) Rao, M.; Berne, B. J. *J. Phys. Chem.* **1981**, *85*, 1498.
(56) Warshel, A. *J. Phys. Chem.* **1982**, *86*, 2218.
(57) Maroncelli, M.; Fleming, G. R. *J. Chem. Phys.* **1988**, *89*, 5044.
(58) Karim, O. A.; Haymet, A. D. J.; Banet, M. J.; Simon, J. D. *J. Phys. Chem.* **1988**, *92*, 3391.
(59) Hwang, J.-K.; King, G.; Creighton, S.; Warshel, A. *J. Am. Chem. Soc.* **1988**, *110*, 5297.
(60) Zhu, S.-B.; Lee, J.; Zhu, J.-B.; Robinson, G. W. *J. Chem. Phys.* **1990**, *92*, 5491.
(61) Carter, E. A.; Hynes, J. T. *J. Chem. Phys.* **1991**, *94*, 5961.
(62) Fonseca, T.; Ladanyi, B. *J. Phys. Chem.* **1991**, *95*, 2119.
(63) Maroncelli, M. *J. Chem. Phys.* **1991**, *94*, 2084.

that both of these effects occur on the same time scale.

Conclusions

There have been several recent time-resolved studies examining the dynamics of excited-state charge-transfer reactions in medium-sized organic molecules.[13,16,17,38] The present study on the intramolecular charge transfer in a series of alkylated (aminophenyl)sulfones suggests that the reaction process involves coupling between torsional (or vibrational) motion and possibly fast solvation dynamics. Following charge transfer, on a slower time scale, solvent orientational relaxation occurs to stabilize the large dipole moment of the TICT state. It is instructive to compare these observations with reports on other molecular systems in an effort to identify unifying features for this class of chemical reactions.

Reported results on the dynamics of DMABN in alcohol solutions arrive at similar conclusions.[17e] This particular molecule has been the subject of numerous theoretical treatments. In the most recent work of Schenter and Duke,[42] is presented a model that accounts for experimentally observed fluorescence dynamics. In order to quantitatively describe the data, the excited-state potential needed to be described as a two-dimension surface, $V(\theta,\mathbf{x})$, taking into account the twisting angle between the amino and phenyl groups, θ, and the solvent polarization, $\mathbf{x}$. Trajectories indicated that the barrier crossing results mostly from motion in the torsional angle. The majority of the solvent relaxation occurs once the TICT state is formed. Similar to the conclusion of the SNM model,[6] the reaction coordinate involves motion in two dimensions and neither a strictly solvent coordinate nor vibrational coordinate model could account for the data. While the dynamics are similar to that observed in the DRAPS system, there is no experimental evidence that the intramolecular mode responsible for the reaction is the twisting motion between the sulfone moiety and one of the dialkylanilino groups.

Both of these cases (DMABN and DRAPS) involve reaction processes that have barriers ($\Delta G^\circ > kT$) along the solvent coordinate. In the limit where the barrier approaches zero, the reaction potential approaches that of a simple relaxation process and the dynamics of the electron-transfer reaction are completely described in terms of solvent motion. Barbara and co-workers have shown that the excited-state electron transfer in BA and ADMA falls within this limit.[26] In particular, the electron-transfer rates for BA correlate with τ_s^{-1} determined from the solvation dynamics of Coumarin dyes in polar solvents.[26a] The steady-state and time-resolved spectra of both molecules could also be quantitatively accounted for by using the semiempirical solvent coordinate model described earlier.[26b,c]

The relative importance of solvation dynamics and vibrational motion in determining the reaction dynamics is dependent on the shape of the excited-state potential and the relative time scales of these molecular motions on that surface. Currently, the molecules being studies are not amenable to detailed calculations of the excited-state potential surfaces. Most theories to date focus on defining expressions for the reaction rate constant. At present, using such theories, it is difficult to define an experimental observable that separates the effects of fast solvation and vibrational motion. Further advances in these areas should make it possible to understand the detailed role of solvent dynamics on electron-transfer reactions.

Acknowledgment. This work was supported by grants from the National Science Foundation and the MMFEL program administered by the Office of Naval Research. J.D.S. thanks Professor R. Marcus and Dr. W. Nadler for many helpful discussions during the early stages of this work. We thank Dr. S.-G. Su for carrying out many of the time-resolved measurements, Professor P. Barbara and Dr. K. Tominaga for help with the spectral modeling, and Dr. H. Kim and Professor James T. Hynes for many helpful discussions.

Registry No. APS, 80-08-0; DMAPS, 33871-62-4; DEAPS, 141018-09-9; DPAPS, 125927-27-7; DBAPS, 125927-28-8.